6 XPD: POWDER DIFFRACTION X-RAY BEAMLINE

6.1 Executive Summary

This chapter describes the design for a damping wiggler based high-energy high-resolution powder diffraction beamline at NSLS-II. This beamline is optimized for high-energy high-resolution x-ray powder diffraction, operating in the energy range from around 20 keV and extending well above 50 keV. This facility will be the only high-resolution instrument in the United States capable of collecting data at high energies and will make it ideal for *in situ* and time resolved studies of samples held in environmental cells. The following sections give a description of the scientific objective of the powder diffraction facility and a conceptual design of the beamline and end-station layout. In proposing a beamline design which could operate effectively, considering the very high power loads that are delivered from the NSLS-II damping wiggler source, the ACCEL x-ray synchrotron beamline design company were hired to arrive at a suitable set of beamline components that would be able to manage these high heat-loads and provide the required optical functions. In this process, a range of scenarios were considered in the design. In this chapter, we highlight our current thinking for such a design, taking some of the concepts and suggestions provided by ACCEL. The scope of this NSLS-II powder diffraction beamline is to provide one high-energy high-resolution x-ray powder diffraction end-station and an additional enclosure for "routine" powder diffraction. This additional enclosure could be equipped with existing NSLS-I equipment and provide an additional facility that could ultimately be served by a canted wiggler source.

6.2 Scientific Objective

The proposed powder diffraction beamline at NSLS-II will be a tunable high-resolution facility with the ability to collect data at high energies (20 keV to 100 keV), offering exceptional capabilities such as fast (milli-second) readout rates and high angular resolution on the same instrument. This will be an outstanding research facility for studying the structure and kinetics of materials under real conditions, and will meet the needs of the powder diffraction user community. For example, there are dedicated powder diffraction facilities at ESRF (BM16, ID31), DIAMOND (I11, I15), APS (sector 16, 5-BM-C, 6ID-B,C,D, 12-BM-B, 33BM-C), SOLEIL (CRISTAL, HighPressure, MARS, SIXS), the Swiss Light Source (MS), and the Australian Synchrotrone. Powder diffraction has widespread scientific interest, such as in the fields of metallurgy, solid-state chemistry, nanomaterials, microelectronics, mineralogy, and the biological and pharmaceutical sciences. In addition, the study of condensed matter at extreme conditions is developing into a very rich field of research. In situ elastic scattering provides the data required to derive structure models, which is essential to systematic searches for new classes of materials and to rationalizing their desirable properties.

The proposed NSLS-II powder diffraction beamline will be the only high-resolution instrument in the U.S. that is capable of collecting data at high energies, which will make it ideal for in situ and time-resolved studies of samples held in environmental cells in which the pressure, temperature, and chemistry can be varied. The high-energy x-rays will be able to propagate through environmental cells, allowing for the investigation of materials made up of high-Z components, and enabling high-q accessibility, which is crucial for atomic pair distribution function analysis and high-pressure cell research. By employing a high-resolution crystal analyzer array, this new instrument will allow enhancement, through suppression of the fluorescence and Compton components (including diffuse scattering), required to evaluate technologically important disordered materials. Due to the inherent small instrumental (and source) broadening, the high resolution of

the crystal array will enable the measurement of accurate peak-profiles, thus allowing the investigation of strain, lattice defects, and micro-structure. The implementation of a fast position-sensitive strip-array detector will also allow the real-time , microsecond timescale study of phase transitions, transformations, and catalytic reactions as a function of temperature, chemical gradients, and pressure. For combinatorial science and screening, robotic sample changers will facilitate rapid sample change and high-throughput data collection.

The great interest and excitement in the proposed NSLS-II powder diffraction beamline was evidenced at the NSLS-II user workshop held on July 17 – 18, 2007, where a breakout session on powder diffraction (http://www.bnl.gov/nsls2/workshops/UserWorkshop_BOS1.asp) was attended by more than 50 people. During this workshop, ideas on the capabilities of the beamline and research areas were discussed. In these early stages of the project, a beamline access team (BAT) is beginning to form and a further workshop is to be held on November 30, 2007.

6.3 Insertion Device

The powder diffraction beamline will be located on a damping wiggler source, which is located in a high-β straight-section of the NSLS-II ring. Unlike the NSLS-II undulator, bending-magnet and 3-pole wiggler sources, the NSLS-II damping wiggler extends the range of high energy x-ray access well beyond the 50 keV region, thus allowing the study of samples under real conditions, i.e. in environmental chambers. The basic parameters for the damping wiggler source used in this design are shown in the tables below Tables 6.1

Table 6.1 NSLS-II Machine and Damping Wiggler Parameters.

NSLS-II Machine & Damping Wiggler Parameters	
Electron energy, Eo	3 GeV
Electron current, Io	500 mA
Number of periods	70
Period length, λu	10 cm
Magnetic field	1.8 Tesla
Deflection parameter, k	16.81
Critical energy	10.8 keV

Table 6.2 RMS Electron Beam Values at the Center of the High-β Straight Section.

Root-Mean-Square electron beam values at the center of high-β straight-section	
Horizontal electron beam size, σ_x	99.0 μm
Vertical electron beam size, σ_z	5.5 μm
Horizontal electron beam divergence, σ_x'	5.5 μrad
Vertical eectron beam divergence, σ_z'	1.8 μrad

We note that as a result of optimization of the damping wiggler design, the period of this device has subsequently been refined to 90 mm. This has the advantage of reducing the angular fan of the radiation, making canting two devices more practical. While this is not expected to have a large impact on the design considerations presented here, it will be necessary to reevaluate any of these issues in light of the new source design.

Figures 6.1 and 6.2 show the flux (integrated over 3 mrad horizontally) and brightness values for the various NSLS-II sources. With a critical energy of 10.8 keV, the NSLS-II damping wiggler has flux values of 1.7 x 10^{15} (at 20 keV), 3.3 x10^{14} (at 40 keV), 5.6x10^{13} (at 60 keV),1.0x10^{13} (at 80 keV) and 1.4x10^{12} (at 100 keV) ph/sec/0.1% BW/mrad. The corresponding brightness values are 2.2x10^{18} (at 20 keV), 1.0x10^{18} (at 40 keV), 5.7x10^{17} (at 60keV), 2.6x10^{17} (at 80keV) and 1.2x10^{17} (at 100 keV) ph/sec/0.1%BW/mrad2/mm^2.

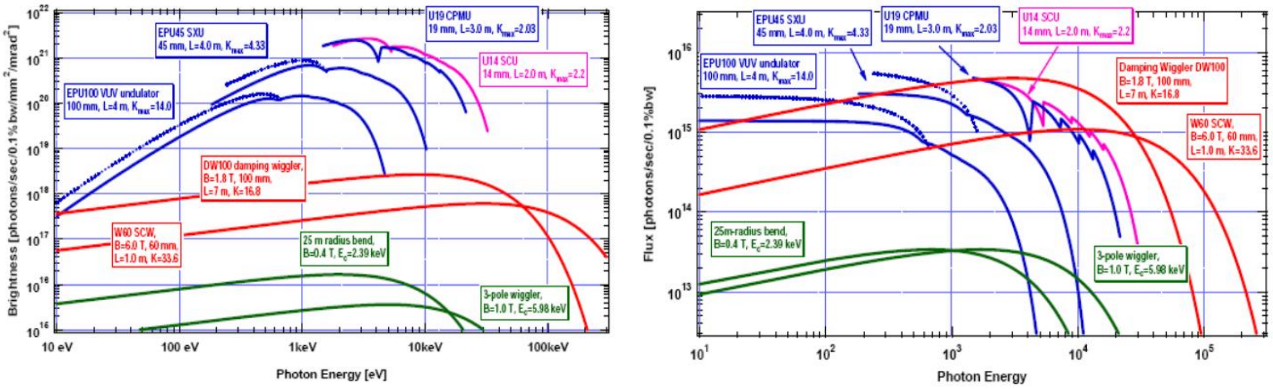

Figure 6.1 Flux and brightness curves for the various NSLS-II sources, including the 7.0m-long damping wiggler source.

Figure 6.2 shows the flux and brightness comparisons between the NSLS-II damping wiggler source and the existing NSLS X17 super-conducting wiggler (a high-pressure diffraction beamline). As is evidenced by these plots, the NSLS-II damping wiggler source exceeds the X17 source output and will make the proposed high-energy high-resolution powder diffraction beamline at the NSLS-II machine a very powerful facility.

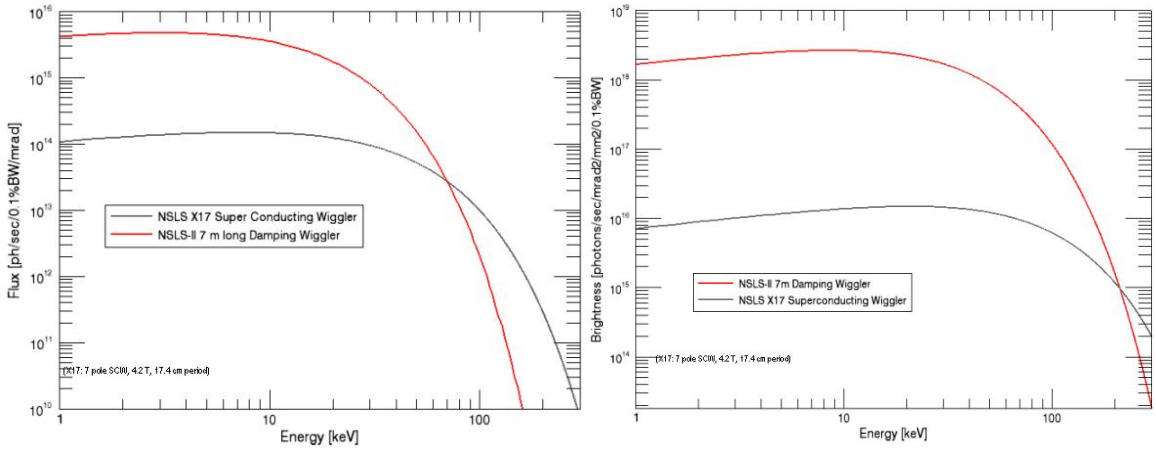

Figure 6.2 Flux and brightness comparisons between the NSLS-II 7m long damping wiggler source and the NSLS-I super-conducting wiggler.

6.4 Sector Layout

The following sections describe the conceptual configuration of the NSLS-II powder diffraction facility.

6.4.1 Front-End Layout

A layout of a typical front-end is shown below (SGV: slow gate valve; FAPM: fixed aperture mask, XBPM: photon BPM; CO: lead collimator; FGV: fast gate valve; SS: safety shutter). The components that are not shown are: 1) ratchet wall collimator (a beam pipe going through the ratchet wall and surrounded by lead), and 2) a gate valve downstream of the ratchet wall collimator (this gate valve can be removed after commissioning).

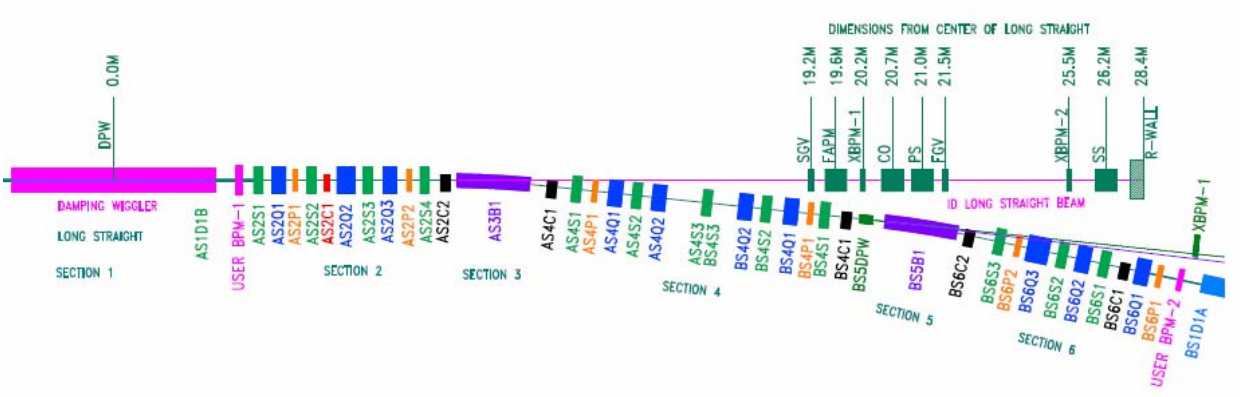

Figure 6.3 Front-end layout plan of NSLS-II.

For the NSLS-II powder diffraction beamline, the fixed aperture mask (FAPM) will limit the angular acceptance to 1 mrad (H) x 0.15 mrad (V) and reduce the power load on the downstream optical components (see Section 6.4.3). In addition, white-beam X-Y slits will be situated between the second x-ray beam position monitor (XBPM-2) and the fast gate valve (FGV), to further reduce power loads and reduce the angular acceptance, if required.

6.4.2 Beamline Layout

From discussions with the user community, potential BATs, and vendors, a conceptual design of the NSLS-II powder diffraction has been devised that would meet the requirements for a high-energy high-resolution facility. Furthermore, the beamline will be designed in way that it allows the addition of a second beamline, which could be served using a second canted wiggler in the same straight section.

Outlined in the tables below are the beamline performance, as described by the various operational modes. All flux values assume a 1mrad (H) x 0.1 mrad (V) acceptance.

Table 6.4 lists the photon flux, in units of ph/sec/0.1%BW, before and after the 1.5m-long Pt-coated vertically focusing/collimating mirror, which operates at a fixed grazing incidence angle of 2 mrad. For operations above 40 keV, where the mirror reflectivity falls considerably, it is withdrawn from the optical path. Reflected in these values are 5 mm of carbon pre-filters.

Table 6.4 Flux at and after the vertical focusing mirror, which is located in the front optical enclosure.

Energy [keV]	Flux at Mirror (with 5 mm carbon) ph/sec/0.1%BW	Flux after mirror (withdrawn for > 40 keV) ph/sec/0.1%BW
20	$4.6x10^{14}$	$3.7x10^{14}$
40	$1.7x10^{14}$	$1.2x10^{14}$
60	$3.7x10^{13}$	
80	$7.2x10^{12}$	
100	$1.3x10^{12}$	

Tables 6.5 and 6.6 detail the x-ray flux, in units of ph/sec, at the sample position (location H in the high-resolution enclosure – Figure 6.4, 57.7 m from the damping wiggler source), using both sagitally-focusing silicon-111 and -311 double-crystal Laue monochromators. The bandpass of these crystal orientations are noted in the table captions. The horizontal focused beam size (FWHM) are estimated from the ~2:1 focusing of this device and current NSLS measurements (see section 6.4.3.3). In the vertical direction, the 1.5 m long mirror in the FOE can deliver a focused 400 μm (FWHM) beam and a 3 of mm beam in the high-resolution/collimating mode, below 40 keV.

Table 6.5 Bent Laue Mode (2:1 focusing): dE/E ~$1x10^{-3}$ – Si(111). 0.5mm-thick Laue crystals and 2mm silicon pre-filter. 5 mm carbon.

Energy [keV]	**Flux at sample** [ph/sec]	**Beam dimensions at sample**
20	1.8x1013	300 μm (H) x 400 μm (V) / 3mm – mirror in
40	1.1x1014	300 μm (H) x 400 μm (V) / 3mm – mirror in
60	3.0x1013	300 μm (H) x 5 mm (V)
80	6.2x1012	300 μm (H) x 5 mm (V)
100	1.1x1012	300 μm (H) x 5 mm (V)

Table 6.6 Bent Laue Mode (2:1 focusing): dE/E ~$1x10^{-4}$ –Si(311). 0.5mm-thick Laue crystals and 2mm silicon pre-filter. 5 mm carbon.

Energy [keV]	**Flux at sample** [ph/sec]	**Beam dimensions at sample**
20	7.2x1012	300 μm (H) x 400 μm (V) / 3mm – mirror in
40	4.4x1013	300 μm (H) x 400 μm (V) / 3mm – mirror in
60	1.2x1013	300 μm (H) x 5 mm (V)
80	2.5x1012	300 μm (H) x 5 mm (V)
100	4.4x1011	300 μm (H) x 5 mm (V)

For very high-resolution powder diffraction work, the Laue crystals can be unbent to eliminate contributions to the vertical beam divergence that can be induced by the sagittal bending. In this mode, the flux and beam size values are shown in Table 6.7. To reduce the horizontal beam size, we propose to use a graded multiplayer focusing optic within the experimental enclosure. Table 6.8 shows both the x-ray flux and beam dimensions for this mode of operation.

Table 6-7 Unbent Laue – for high resolution. dE/E ~1x10^{-4} – Si(111)

Energy [keV]	**Flux at sample** [ph/sec]	**Beam dimensions at sample**
20	1.8x1012	5.8 cm (H) x 400 μm (V) / 3mm – mirror in
40	1.1x1013	5.8 cm (H) x 400 μm (V) / 3mm – mirror in
60	3.0x1012	5.8 cm (H) x 5 mm (V)
80	6.2x1011	5.8 cm (H) x 5 mm (V)
100	1.1x1011	5.8 cm (H) x 5 mm (V)

Table 6.8 Unbent Laue – for high resolution. dE/E ~ 1x10^{-4} – Si(111) + 0.5mm-long graded multiplayer optic.

Energy [keV]	**Inc. Angle** [mrad]	**Hor. Accep.** [mm]	**Flux at sample** [ph/sec]	**Beam dimensions at sample**
20	7.7	3.15	9.8x1010	14 μm (H) x 400 μm (V) / 3mm – mirror in
40	3.9	1.95	3.7x1011	14 μm (H) x 400 μm (V) / 3mm – mirror in
60	2.6	1.3	6.7x1010	14 μm (H) x 5 mm (V)
80	1.9	0.95	1.0x1010	14 μm (H) x 5 mm (V)
100	1.5	0.75	1.3x109	14 μm (H) x 5 mm (V)

The conceptual layout for the NSLS-II powder diffraction beamline is shown in Figure 6.4. The beamline consists of the following optical components:

A. a pre-filter and beryllium window – to isolate the beamline from the machine vacuum, and a filter unit to limit the power load on the downstream optical components

B. a 1.5 meter long bendable focusing/collimating mirror operating at a fixed grazing incidence angle of ~ 2mrad, which will be coated with platinum and be able to function up to 40 keV. Above this energy, this mirror will be withdrawn from the optical path

C. a sagitally focusing double-crystal Laue monochromator to provide focusing and wavelength selection, with the required band-pass

D. beam monitoring unit

E. a monochromatic photon beam shutter

F. sample position in the upstream experimental hutch (endstation equipment not in the scope of this project)

G. a horizontal focusing graded multiplayer for focusing the beam onto small samples at H

H. a sample position in the downstream experimental enclosure

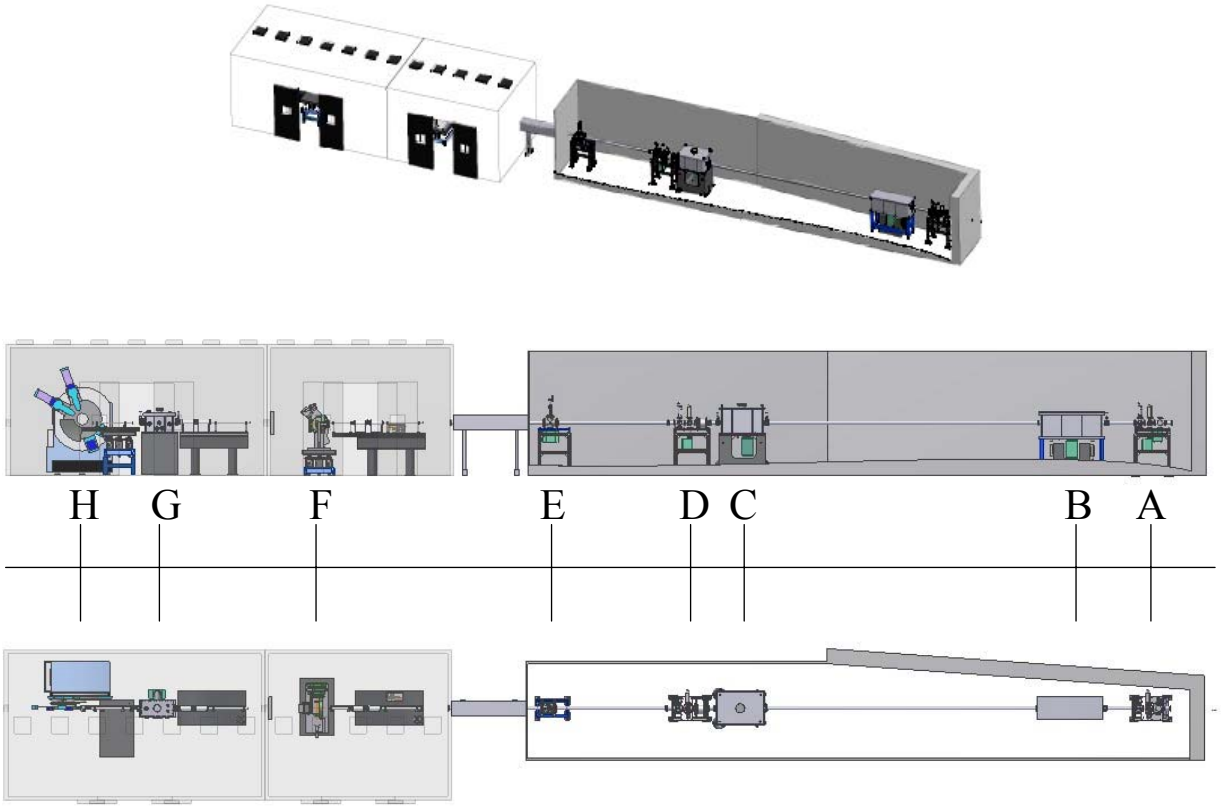

Figure 6.4 Conceptual layout for the powder diffraction beamline.

Table 6.9 Distances of the various components from the conceptual layout of the powder diffraction beamline.

Component	Distance from Source
A. Be window and Filter Unit	29.0 m
B. 1.5m-long focusing/collimating mirror	31.1 m
C. Sagitally Focusing Double-Crystal Laue Monochromator	40.0 m
D. Beam Monitoring Unit	41.36 m
E. Monochromatic Photon Shutter	45.1 m
F. Upstream Sample Position	51.3 m
G. Horizontally Focusing Graded 0.5 m long Multilayer	55.6 m
H. Downstream Sample Position	57.7 m

6.4.2.1 Survey and Alignment Plans

All beamline components will be surveyed and aligned in place by the facility. To facilitate ease of alignment, all components will be fiducialized to external reference points on their table during assembly. All components are designed with a liberal tolerance allowance greater than 0.5 mm.

6.4.2.2 Utility Layouts

Cooling water is required for all high-heat components. Requirements for the standard cooling water supply and the components and flow rates that are needed are shown in the tables below.

Table 6.10 Cooling water requirements for the XPD.

Approximate Temperature	20°C to 30°C
Temperature Stability	± 1°C
Maximum Pressure	6 bar
Pressure Stability	± 0.1 bar
Quality	de-ionized but not ultra-pure

Table 6.11 Flow requirements for the various XPD optical components.

Component	# of Circuits	Max. Consumption
Pre-Filter and Be window	1	4 l/min
Attenuator Units	4	8 l/min
Vertical Collimating/Focusing mirror and mirror protection mask	1	12 l/min
Thermal Stabilization and Cooling of Laue mono	1	Local Chiller
White Beam Stop	1	4 l/min

The cryo-cooler unit for the double-crystal Laue monochromator requires connection to a liquid nitrogen supply. It is recommended to have a liquid nitrogen supply within 2 to 3 meters of the final cryo-cooler position. The following components must be connected to a dry, filtered compressed air supply having a pressure of between 70 psi and 100 psi: the monochromatic photon beam shutter, all gate valces and the pneumatically driven attenuator filter units. There are three main areas where electrical power is required:

- Control system cabinets: A central 3-phase power distribution should be placed near the cabinets. In total, approximately 12 kW are required,
- Cryo-cooler unit: This unit needs a 1-phase power distribution of approximately 2.5 kW,
- Enclosures:

Within the hutches, two types of power outlets should be provided for each section: a low-noise outlet for measuring equipment and a standard outlet for mobile pumps and heaters. The outlets should be distributed along the length of each enclosure. The required power in the front optical enclosure could be up to 30 kW to accommodate the extreme case where the full beamline may be pumped and baked at the same time. Along the beamline a grounding bar is needed, to ground the beamline components. The grounding bar must be connected to the central power distribution ground.

6.4.2.3 Beamline Vacuum System

We have assumed that there will be several vacuum sections, isolated from each other through gate valves. Each vacuum section will be equipped with one ion pump and has one rectangular all-metal valve, CF40, to rough down the vacuum using a pump cart and to vent the section. The monochromator is equipped with one all-metal valve CF16 for venting and, in addition, with a CF63 gate valve where a turbo molecular pump will be permanently mounted. Each section is also equipped with a full-range vacuum gauge. The white

beam part of the beamline will be realized to be bakeable in order to achieve a vacuum pressure below 10^{-9} mbar. The monochromatic part is designed to achieve a base pressure in the 10^{-8} mbar range. Besides the large flanges of the monochromator doors (that are Viton sealed) and of the mirror vessels (metal sealed for the VCM and Viton sealed for the VFM) all flanges will be realized according to the Conflat standard.

The layout of a typical vacuum system for one beamline section, and a general overview of the entire vacuum and EPS systems are shown in Figure 6.6.

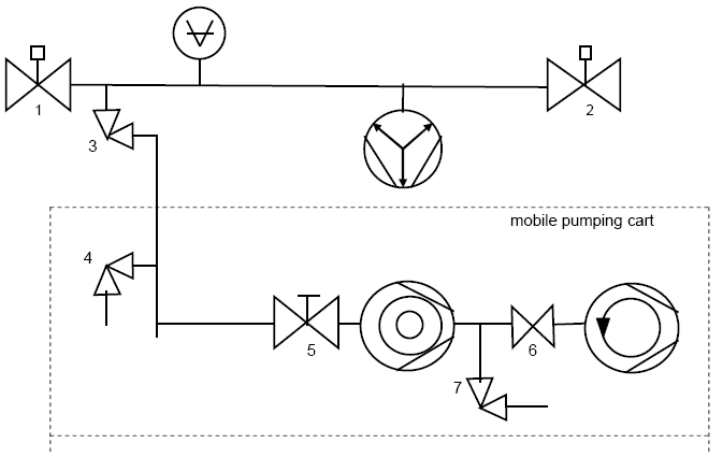

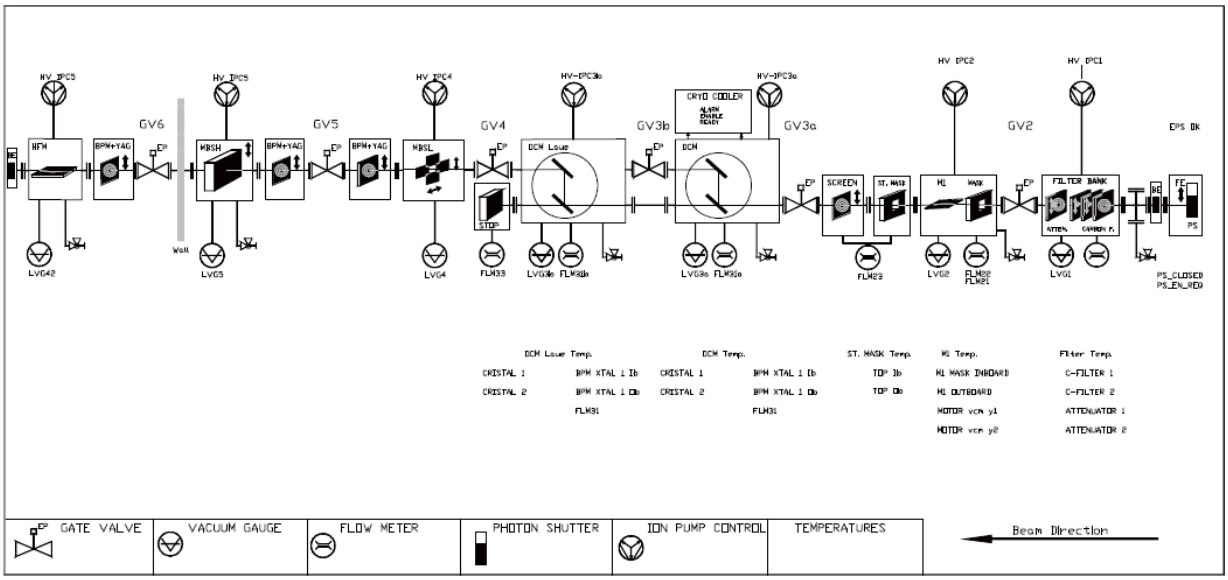

Figure 6.6 **Top**: 1,2 : Sub-section isolation valves. 3: full metal right-angled valve attached to the BL-section. 4: Right-angled valve to vent either the sub-section or the pumping station. 5: hand actuated gate valve CF63. 6: valve to separate the pre-pump from the leak detector. 7: valve to connect the leak detector. **Bottom**: General schematic overview of the entire vacuum and EPS system. The DCM indicated in the drawing is from earlier design considerations, and does not exist in the current configuration.

6.4.2.4 Beamline Control, Motion Control, and EPS

This section covers a general specification for a beamline control system, including the Equipment Protection System (EPS) and the vacuum controls as it could be realized for a NSLS-II beamline. The particular control system chosen here is based on Delta-Tau hardware and Experimental Physics and

Industrial Control System (EPICS) software. The EPS is based on a PLC unit and covers the vacuum monitoring and control as well. This document provides the specifications for the design of a typical beamline control system (BLCS). The beamline control system is the electronic hardware and software interface between the beamline operator and the beamline components. It must be versatile and robust to allow the operator reliable remote control of the beamline components and endstation hardware for the purpose of aligning the beamline and conducting experiments in a precise and yet safe and protective way. It should also have the capability of easily implementing high-end automation. The complete BLCS for the beamline consists of the software and hardware for the following subcomponents:

- control of the full beamline (through EPICS IOCs)
- motion control
- beamline diagnostics
- vacuum control
- beamline equipment protection system (BLEPS)
- control of the closed-loop cryo-cooler

The overall hardware and software architecture is determined by the use of EPICS for beamline control. Within this architecture, field I/Os (i.e., signals from beamline components, experimental stations, etc.) are concentrated in controllers called EPICS IOCs. There can be several EPICS IOCs per beamline. These IOCs communicate to EPICS channel access clients (operator workstations), other EPICS IOCs and embedded EPICS IOCs using TCP/IP. Through these IOCs, the control of the motion of the component axes, detectors, feedback, interfacing to the BLEPS, etc. is established. From an EPICS client, a user can remotely operate the beamline through operator interfaces. Previous releases of EPICS Base required that EPICS IOCs use a vxWorks operating system. However, EPICS Base Release 3.14 has allowed the configuration of operating systems such as Unix, Linux, and Windows as EPICS Soft IOCs. With this configuration, use of non-VME hardware is now possible, lending greater flexibility in the choice of control hardware.

6.2.4.5.1 Overall Beamline Control

The BLCS uses many hardware and software interfaces to establish communication between the various devices that constitute the beamline. The design of the BLCS aims to combine the advantages of having centralized control for convenience of software maintenance and upgrade and yet distributed intelligence for more flexibility, better cable management and housekeeping. All cabling from the beamline components can be routed to control cabinets located near the optics and hutch. Figure 6.7 shows a possible layout of the beamline control devices and the communication interfaces.

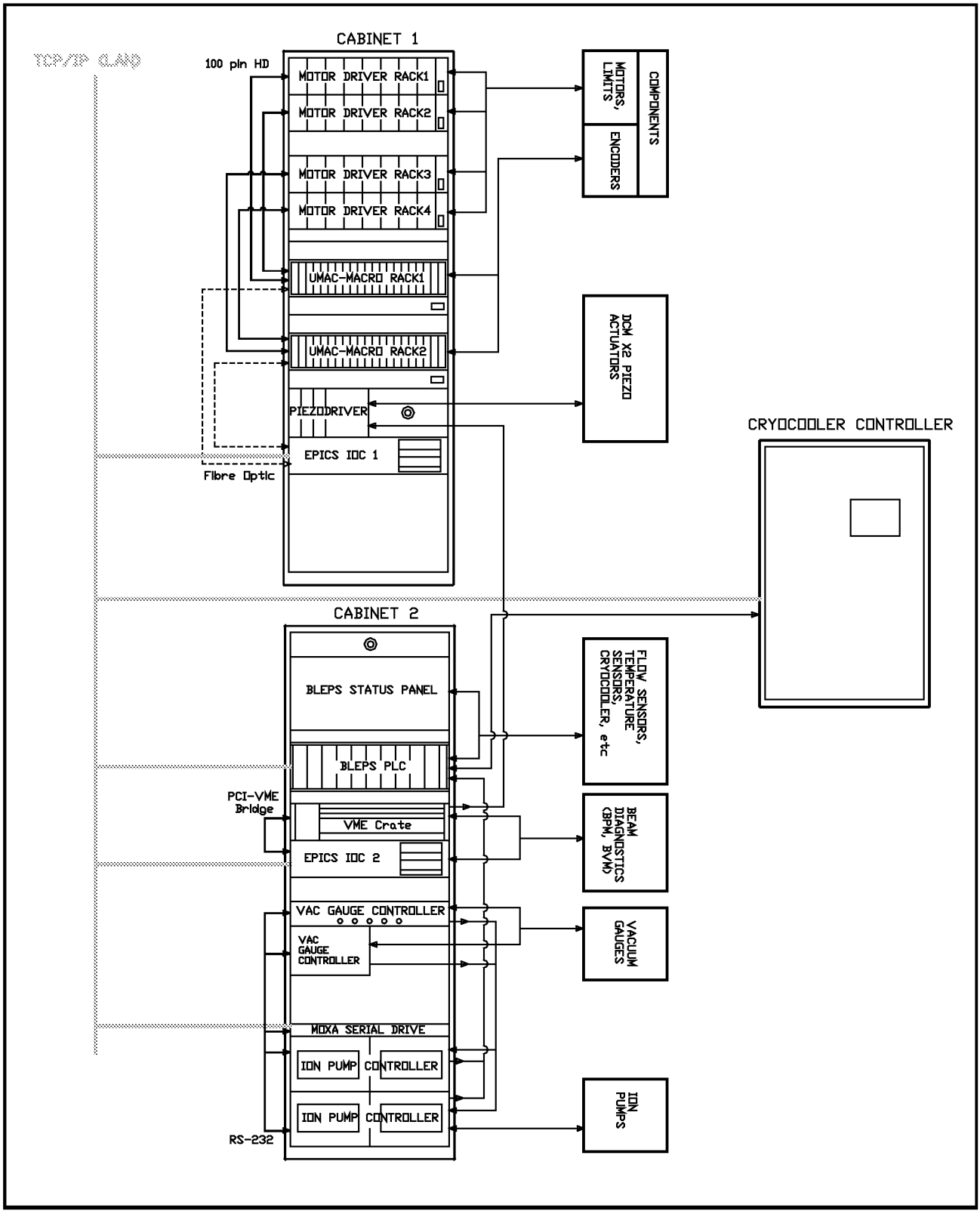

Figure 6.6 Possible layout of the powder diffraction beamline control system.

The beamline control hardware will be housed in two 19-in. control cabinets or racks. The cabinets will consist of several control crates where a crate is a 19-in., variable-height enclosure. The crate types are listed in Table 6.11.

Table 6.11 Possible Crate Control Configurations for the Powder Diffraction Beamline.

Crate	Function
EPICS IOC	A workstation PC running a Linux O/S and configured as an EPICS SoftIOC. It will have PCI slots populated with the motion controller and signal processing cards.
UMAC MACRO Crate	The distributed interface to the stepper motor drivers, encoders, motion control related DIO and AIO
Stepper driver crates	8-axes stepper driver crates
Piezo controller	Control for the piezo actuators
BLEPS	The BLEPS PLC, I/O modules and Status Display Panel
Vacuum gauge control	For readout of the vacuum gauges installed on the beamline
Ion pump controllers	Each controller serves two ion pumps. Two controllers occupy 19-in. x 3HU.
MOXA Serial Drive	Provides serial ports for communication of serial devices with the EPICS IOC. It communicates with the EPICS IOC through TCP/IP.

Each cabinet has an input power requirement of 3-phase/400VAC, 20A. The 3-phase supply is broken out into three single-phase 230VAC supplies within the cabinet which powers the instrumentation crates.

The cryo-cooler control unit will be a stand-alone unit comprising all the control electronics for controlling and monitoring the liquid nitrogen cryo-cooler. It will contain its own PLC for signal processing and alarm handling and will communicate with the beamline EPS through TCP/IP (and hardware connections, if required) to perform specific safety interlock tasks. It will also have a local control/status panel for constant monitoring independent of the network.

These are local electronics that need to be located close to components and are mounted onto the support structures of the components. Local electronics include interpolators for electronics and LVDT readouts. The LVDT readouts output 0-10 V analog signals which will be routed to an ADC readout in the control cabinet.

The beamline will be controlled through EPICS. The EPICS environment will consist of: 1) IOCs running Linux, 2) EPICS Base 3.14.7 or higher, and 3) State Notation Language/Sequencer sequence programs: MEDM and EDM, other EPICS extensions as required, and SynApps.

The control hardware used in the powder diffraction beamline should be supported through EPICS device driver and device support modules. Purely soft support modules are also required to provide useful functions such as data acquisition, scanning, save/restore, user calculations, etc. Through these modules a user, sitting at an EPICS client, can communicate with the EPICS IOCs, the EPICS IOCs can communicate with the control hardware, and the hardware components communicate with each other. The operator interfaces will be the GUIs through which a user operates the beamline. GUIs will be developed with MEDM or EDM.

Beamline motion control refers to the control of all the movable axes of the beamline, the readback of the encoding elements, and the activation of protective switches that limit over-travel. Furthermore, when incremental encoders are used, homing mechanisms should be incorporated for calibration of the absolute position of the axis. Motion control hardware includes the following: 1) motion controller system, 2) motor amplifiers/drivers, 3) connection hardware (interface panels, connectors, cable), 4) Limit/Home switch hardware, and 5) encoder hardware.

For motion control hardware, we are considering the intelligent motion controllers from Delta Tau due to their excellent performance for synchronized correlated motions and for their flexibility. The MACRO[1] distributed system consists of two 32-axis motion controllers residing in PCI slots of the EPICS IOC1, connected through fiber optics to UMAC-MACRO crates. These UMAC-MACRO crates can be customized to output signals supporting several types of motors, digital and analog I/Os, and encoder inputs.

Each 19-in. UMAC-MACRO crate can support up to 32 motorized axes. Each set of eight axes in the UMAC-MACRO connects to one eight-axis motor driver crate. The Turbo PMAC2 PCI Ultralite is a member of the Turbo PMAC family of boards optimized for interface to the system through the MACRO ring. It can command up to 32 axes through the MACRO ring. The Turbo PMAC2 PCI Ultralite is a full-sized PCI-bus expansion card. This card is capable of PCI bus communications, with or without the optional dual-ported RAM (DPRAM).

For this beamline control, the card will be delivered with the DPRAM option. Standalone operation is also possible, and communications can occur through an RS-232 port. Through the rest of this chapter, the 32 axis PMAC2 motion controller will be referred to as the PMAC. MACRO is an acronym for Motion and Control Ring Optical and is a non-proprietary digital interface developed by Delta Tau for a single-wire connection between the multi-axis motion controllers, amplifiers, and I/O through a fiber optic ring. The MACRO minimizes wiring complexity, reduces hardware, and eliminates noise in large systems. The high-speed 125 Mbits/sec transfer rate is capable of closing the servo loops across the MACRO ring, allowing the flexibility to choose distributed intelligence or centralized control. The 16-axis UMAC MACRO CPU provides a remote interface for encoders, flags, direct-PWM digital drives, analog drives, and/or digital I/O for a Turbo PMAC2 with MACRO interface. It communicates with the Turbo PMAC2 solely through the MACRO ring, but interfaces to standard drives, encoders, flags, and Opto-22 style I/O through on-board connectors. It is designed to run up to 16 motors. Through the rest of this chapter, the 16-axis UMAC MACRO CPU will be referred to as the UMAC.

An interface board between the UMAC-MACRO Crate and the Stepper Driver Crate forwards the step/direction signals and returns the limit/flag signals. Each board provides signals for eight axes and connects to the stepper-driver crate through a standard 100-pin, high-density connector. This interface board will be mounted on the rear of the UMAC-MACRO crate.

Bipolar stepper drivers will be provided to match the requirements for the specific axis in terms of torque requirements, drive currents, and micro-stepping. All motorized axes on optical components (monochromator and mirrors) and slit systems will be encoded with incremental encoders (quadrature or analog). All motorized axes will be fitted with limit switches to determine the travel range and to protect against mechanical damage caused by over-travel. These switches are externally mounted and can be adjusted to set a required travel range. The limit switch contacts are configured to be “normally closed.” Homing of the component axes, to zero the counter, is performed using the precision end switches. Table 6.12 lists typical types of cables and connectors.

Table 6.13 List of possible cables and connectors for the powder diffraction beamline.

Function	Cable Type	#CondPairsxCross-section	Connector
Motor	Facility standard	4x2x0.75mm^2 + 6x0.25mm^2 (separately shielded)	Trim-Trio Souriau e.g. UTO014-12ST
EPS SIGNALS	Unitronic LiHCH (TP)	4x2x0.25 12x2x0.25	SubD-9 (valves, flow, pressure) SubD-25 (temperatures)
Quadrature ENCODER	Unitronic LiHCH (TP)	8x2x0.25	SubD-15
Analog Encoder	Belden 8164	4x2x0.23	SubD-15
D/A/Video SIGNALS	Coxial	RG58U, RG174	BNC, Lemo

[1] Motion and Control Ring Optical

The motion control software is determined by the use of the Delta Tau motion controller and the EPICS control software. PMAC Executive Pro Suite is a Windows-based suite of programs, running on Windows XP and 2000, that communicates to the PMAC through its serial port. It allows standalone operation of the motion controller for initial configuration of the hardware and for testing of connections to the stepper drivers. It also contains tuning and plotting programs useful for performance demonstration and debugging at a lower level. Uploading and downloading of files and variable settings is possible for quick configuration and saving/restoring of settings.

The EPICS support for the PMAC2 controller will also contain a set of setup files that must be downloaded to the PMAC. These files are not EPICS specific but are required to set up the communication of the EPICS IOC to the controller. They will be preloaded to the PMAC/UMAC prior to establishing EPICS communication. As mentioned before, our design is based on control of the motion of the component motors though EPICS through the support developed for the Turbo PMAC2 PCI Ultralite motion controller currently in use at the XAS beamline at the Australian Synchrotron.

Beam position monitors will be installed along the beamline as diagnostic elements. To read out the current signals from these monitors, use of compact quad-electrometer electronics are considered. These devices are supported in EPICS and can be used to feed back the BPM signal to a piezoelectric actuator via a 16-bit DAC. They can also be used for ion chambers.

There will be beamline vacuum control and monitoring instrumentation, consisting of a vacuum gauge controller, the Pfeiffer Maxiguage TPG256A, and the ion pump controllers. The vacuum gauge controller and the ion pumps will interface to the EPICS IOC via their RS232 ports. RS232 ports are provided by the MOXA Nport5610-8 serial device server which communicates to the EPICS IOC via TCP/IP. Vacuum level readouts from the vacuum gauges will be input into the vacuum controller which will compare the readings against preset trip points. Status of these trip points are directly wired to the BLEPS as digital inputs. The status of the HV of the ion pumps is directly monitored by the BLEPS. Through EPICS, the pressures read by the vacuum gauges will be remotely available.

The primary purpose of the beamline EPS is to protect the individual beamline components against x-ray damage, loss of vacuum, loss of coolant flow (water and liquid nitrogen), and elevated temperatures. The beamline EPS communicates with the Beamline Personal Safety System (BLPSS) PLC and with the Front End EPS and Front End PSS (FEEPS, FEPSS) through specified interface signals. Communication to the EPICS IOCs is via modbusIP. The EPS hardware will be based on the Programmable Logic Controller (PLC) technique (e.g., Schneider Electric TSX Premium), including a CPU (TSXP572634M) with an Ethernet interface. The BLEPS hardware will consist of an approximately 4HU 19-in. crate (CPU and I/O modules) and a 6HU local display panel. The display panel will be an etched aluminum plate with green/red LEDs to indicate satisfactory/unsatisfactory conditions of the relevant component signal. The BLEPS PLC will be programmed to take protective actions in the case of detection of unfavorable conditions in the beamline.

Control and monitoring of the PLC will be available through GUIs and will offer the following functions: 1) Monitoring: EPS alarm status, beamline gate valve status, temperature values, flow trip points status, pressure trip point status, ion pump HV status, cryo-cooler ready/alarm/enable status, pneumatic actuator position status, and conductivity meter readings; and 2) Control: beamline gate valves and pneumatic actuator insertion/retraction.

For ease of configuration of the BLEPS, the beamline will be divided into EPS vacuum sections. The vacuum sections are defined based on the specific beamline component configuration and the need to isolate the components. Vacuum sections are bounded by gate valves. Based on information on the beamline design and requirements for communication with other sections of the beamline control system, interface signals will be determined. All relay contacts are “normally open” (N/O), 24 VDC Flag return signals. In general, the following type of beamline signals will be monitored by the BLEPS: process cooling water (PCW) flow, conductivity, critical device temperatures (filters), fixed and “disaster” masks,, monochromator crystals, vacuum, cryo-cooler status, gate valves position, pneumatic-driven filters, and beam position monitors.

The cryo-cooler controller is a stand-alone control cabinet which controls the closed-loop liquid nitrogen circuit used to cool the monochromator Laue crystals. It interfaces to the EPICS IOC for remote monitoring and control and to the BLEPS for communication of ready status and alarm signals.

6.4.3 Beamline Components

The following items describe the various beamline components for the high-energy, high-resolution powder diffraction beamline.

6.4.3.1 White Beam Slits

These components are included in the front end (Section 6.4.1), thus they do not belong to the scope of supply for the beamline.

6.4.3.2 Pre-Filter, Beryllium Window, and Attenuators

In hard x-ray beamlines, one typically uses a beryllium (Be) window to separate the beamline vacuum from the machine vacuum. Such a window has also the advantage that it absorbs a good fraction of the unused low energy x-ray spectrum, therefore reducing the overall power dumped on downstream components. However, in a wiggler beamline such as the NSLS-II DW 100 described here, calculation of the absorbed power indicates that a Be window in the direct of white beam from the wiggler simply would fail. Due to carbon's high thermal conductivity and mechanical stability, carbon foil(s) is (are) typically used as a protective filter material in front of or instead of a Be window. The combination of carbon filters and Be windows must be carefully tailored, taking into account both the absorbed heat load and the requirement for the highest possible flux transmission at lower energies. Our approach is to design a filter assembly that can be safely used whenever required, to reduce the power levels on the optical components.

Reduced power always will improve the performance of white beam optical components such as the focusing/collimating mirror and the sagitally-focusing double-crystal Laue monochromator. Considering the high heat load that is produced by the wiggler, the carbon filter unit is an essential component for maintaining sustainable power levels along the powder diffraction beamline. With respect to the heat load absorbed by the most upstream filter, a standard water-cooled graphite filter cannot cope with the high heat load. From experience at other facilities using similar powerful sources, we considered two possible solutions: 1) Using thin C foils which are only radiation cooled. In that case the foils become extremely hot – up to 1500°C and higher. 2) Using high-thermal-conductivity highly oriented pyrolytic graphite (HOPG) foils to form a filter frame, which can be safely water cooled.

In the following paragraphs some proven designs are summarized:

ALS, Beamline 5.0[2]

HOPG is clamped between two water cooled copper frames and absorbs 10 W/mm^2 (250 μm). The contact pressure is finely adjusted by springs. Temperatures up to 1000K are possible. After more than one year operation, there is no visible damage on the HOPG foil.

NSLS, MGU-undulator-beamline[3]

A stack of radiative cooled foils successfully withstand the power load from a wiggler (3.4 W/mm^2). They use seven foils, starting from 5 μm up to 51 μm. After a few years of operation, no visible damage can be observed on the foils. In addition it has been verified that the temperature of the foils is somewhat lower

[2] Private communication with D.Cambie; "Annealed Pyrolytic Graphite filter for beamline 5.0 at the ALS" - D.Cambie, C.Cork – MEDSI proceedings 2004

[3] private communication with P. Montanez and L. Bermann

than the calculated value. This system has proven to work reliably up to temperatures of 1000°C and slightly higher.

CHESS, wiggler-beamlines[4]

A HOPG foil was brazed directly to a copper block (12 W/mm^2 on 250 µm). Some cracks observed in the foil most likely were caused by the cooldown process during brazing. The system worked for some time, but failed with doubled power load. The replacement design has operated without failure for several months. The HOPG is clamped on two sites in a copper frame with improved water-cooling performance (jet-stream-cooling, very closed to the edge of the HOPG).

The consultant evaluated the behavior of the first filter unit for the power load of the damping wiggler source (please refer to Appendix D), demonstrating that both options, radiation-cooled filter elements as well as contact-cooled filters, are possible solutions for this beamline. A final careful FEA must be carried out using the final source parameters. In the beamline design they incorporated two components, a Be-window with sufficient pre-filters and an attenuator set up to manage the power load on the optical components:

6.4.3.2.1 Pre-Filter

This component is very similar to the setup already in use at several beamlines at BNL. It consists of a water-cooled frame that holds the different filters. The radiation-cooled foil is held in a tantalum frame, since it must withstand the extremely high contact temperature, and will become hot itself. The power then is dissipated into the surrounding environment and is absorbed by a water-cooled copper surface positioned around the tantalum frame. The tantalum frames, together with the carbon foils, are placed in a water-cooled cartridge made of OFHC copper. The cartridge is held and mounted on a DN40CF flange. The assembly is mounted to a DN100CF base flange and fits in a DN100CF standard cross. PT100 temperature sensors (e.g., two sensors) will be installed in the copper cartridge and monitored by the control system. If any PT100 sensor exceeds a temperature limit, the beam shutter will be closed. The PT100 sensors will be connected to an electrical feed-through. The water pipe (SF-copper, Ø8x1) will be brazed on the cartridge and on a DN40CF flange, avoiding water-to-vacuum joints. Possible carbon filter combinations are shown in Table 6.14.

Table 6.14 Possible Carbon Pre-Filter Combinations for the Be Window.

Filter no.	Filter thickness [µm]	absorbed power [W]	absorbed power density [W/mm²]
1	5	222	1.6
2	5	96	0.7
3	5	72	0.5
4	25	240	1.8
5	25	162	1.2
6	50	237	1.8
7	50	180	1.4
8	100	277	2.1
9	135	283	2.2
10	300	457	3.6
11	300	337	2.6

[4] private communication with J.Savino; “Improved high heat load graphite filter design at CHESS wiggler beamlines” – J.J.Savino, Q.Shen – SRI 2003 Proceedings

6.4.3.2.2 Attenuator Unit

This unit consists of a number of different filter setups that allow tailoring the power load on the optical components to the right level of operation for each particular operational mode of the beamline. The design being considered is based on one built recently by ACCEL for other high heat load beamlines and is described in the following paragraphs. Currently, we assume that for the DW beamlines it might be reasonable to work with two pneumatically driven attenuator units and two, or even three, motorized filter banks with different filters mounted. The latest design is based on a series of three water-cooled filters mounted on three pneumatic drives. These three carbon foils are of annealed pyrolytic graphite (APG). The foils have a thermal behavior similar to that of HOPG and are available down to thicknesses of 50 μm. The foils are clamped to copper frames where the thermal contact is improved by 1) polishing the surface of the copper within the contact area and 2) using springs that apply a wel-defined and well-distributed contact pressure. The thermal conductivity of APG is similar to diamond. Due to its excellent mechanical properties, and together with the advanced cooling, each foil is designed to remove about 500 W. The power density on the first foil constitutes the biggest challenge and therefore limits the maximum thickness of the foil, while heat conduction as well as physical integrity under thermal stress define its minimum thickness. The APG foil used in the existing system is 125 μm thick. The second foil can only be inserted in the beam when the first foil is already in place.

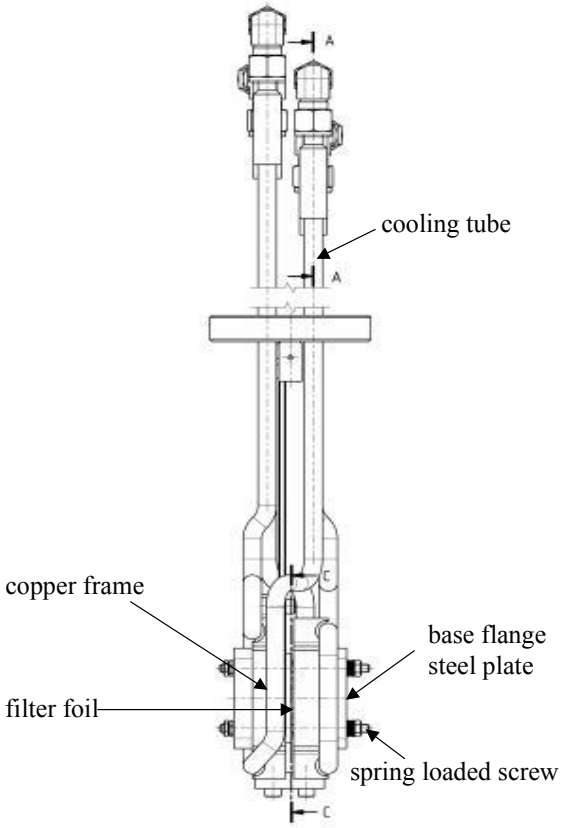

Figure 6.xx Directly-cooled high-power filter set-up, pneumatically driven.

The fourth filter drive is motorized and consist of a cooled frame with five positions that can be used for graphite foils (pyrolytic graphite) of different thickness to be used to further attenuate the beam. This filter design avoids water-to-vacuum joints. Water pipes are brazed to each cooled copper frame and to the vacuum feed-through, where edge-welded bellows allow the translation of the frames with the filters.

6.4.3.3 Sagitally-Focusing Double-Crystal Laue Monochromator

Sagittal focusing using Laue crystals was pioneered at the NSLS (Zhong et al., 2001; Zhong et al., 2002; Zhong et al, 2003). The concept is shown in Figure 1a. This new x-ray optics concept makes it possible to focus a large divergence of high-energy x-rays produced by the NSLS-II damping wiggler. The extent of such focusing is similar to that of sagittal focusing by a Bragg crystal, except for a factor related to the asymmetry angle. The anticlastic bending facilitates the use of inverse-Cauchois geometry in the meridional plane to provide better energy-resolution and to increase the photon flux by an order-of-magnitude compared to traditional sagittal focusing with Bragg crystals. Furthermore, sagittal focusing by a Laue crystal is preferred over a Bragg crystal at x-ray energies above 30 keV because, unlike Bragg crystals, the length of the beam's footprint on a Laue crystal is small and insensitive to energy. For many experiments, beam divergences of order 1 milli-radian at the sample will be tolerable. In diffraction experiments with a vertical scattering plane geometry, a larger divergence in the horizontal plane can also be tolerated.

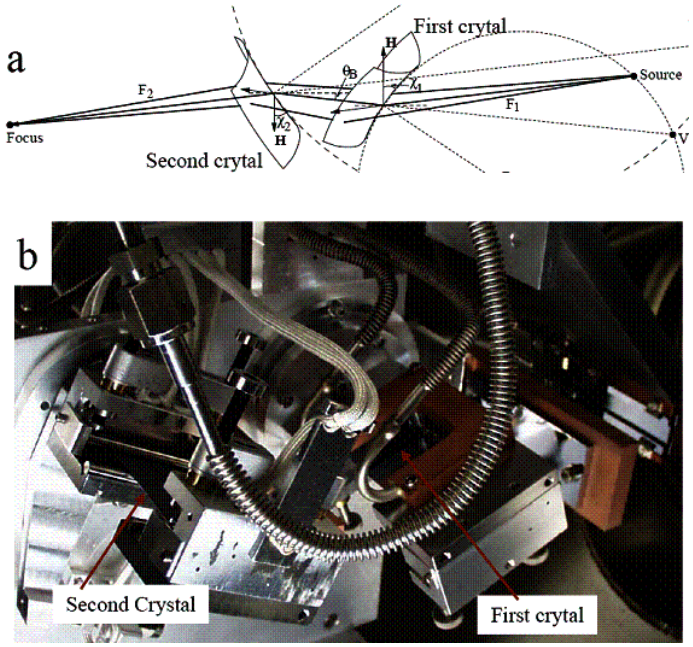

Figure 1: The mechanism of the sagittal focusing with asymmetric Laue crystals, bending of the crystals causes precession of the diffraction vector (H) around the axis of sagittal bending, and the resulting focusing of the diffracted beams. b) Photograph of a monochromator installed at the NSLS X17B1 beamline.

A double-crystal sagittally focusing monochromator, based on this concept, has been constructed and tested, and has been in use at the X17B1 beamline for two years, providing 67 keV x-rays (Figure 1b). It focuses a horizontal divergence of 3 milli-radians to a brightness-limited horizontal dimension of 0.2 mm. The x-ray flux-density at the focus was a few hundred times larger than that of unfocused x rays. Currently, using this device, flux on a small sample in a diamond-anvil cell is limited by the brightness of NSLS storage ring.

1. Z. Zhong, C. Kao, D.P. Siddons, H. Zhong, and J.B. Hastings, "X-ray reflectivity of sagittally bent Laue crystals", *Acta. Cryst. A* **59** (2003) 1-6.
2. Z. Zhong, C. Kao, D.P. Siddons and J.B. Hastings, "Rocking-curve width of sagittally bent Laue crystals", *Acta Cryst, A* **58** (2002) 487-493.

3. Z. Zhong, C.C. Kao, D.P. Siddons and J. B. Hastings, "Sagittal focussing of high-energy synchrotron x-rays with asymmetric Laue crystals, II: experimental studies", *J. Appl. Cryst.*, **34** (2001) 646-653.
4. Z. Zhong, C.C. Kao, D.P. Siddons and J. B. Hastings, "Sagittal focussing of high-energy synchrotron x-rays with asymmetric Laue crystals, I: theoretical considerations", *J. Appl. Cryst.* **34** (2001) 504-509.

After reviewing the current status of the sagitally-focusing double-crystal Laue monochromator, we do not expect any major technical difficulties to realize a final version of the device that could be integrated in the powder diffraction beamline, apart from the management of the rather large heat load expected on the set of necessary C and Si pre-filters, and also on the first crystal itself, and on the white beam stop that has to be positioned in between the two diffracting elements. In order to get a quantitative feeling of the challenges related to the large heat load inherent to the damping wiggler source, we have carried out a preliminary study focused on what could be reasonably thought to be the worst-case scenario: a full 7 m long damping wiggler and the maximum acceptance of the beamline of 1 (hor) x 0.15 (ver) mrad^2. Results are detailed in **Table 6.14 Power load on filters and crystals, on the powder diffraction beamline, for a fixed acceptance of 1 (hor) x 0.15 (ver) mrad^2.**

C Pre-filter thickness [mm]	Si Filter thickness [mm]	Power absorbed in C Pre-filter [W]	Power absorbed in Si Filter [W]	Power absorbed in first Laue Xtal [W]	Power dump in beam stop [W]
2	0	3331	0	1642	2435
2	1	3331	2246	354	1477
2	2	3331	2840	177	1060
3.5	0	4057	0	1182	2169
3.5	1	4057	1691	310	1350
3.5	2	4057	2215	159	977
5	0	4560	0	907	1941
5	1	4560	1341	271	1236
5	2	4560	1803	143	902
10	0	5578	0	457	1373
10	1	5578	724	180	926
10	2	5578	1037	102	691

and **Error! Reference source not found.** below.

Power load on filters and crystals for a fixed acceptance of 1x0.15 mrad^2 :

Table 6.14 Power load on filters and crystals, on the powder diffraction beamline, for a fixed acceptance of 1 (hor) x 0.15 (ver) mrad^2.

C Pre-filter thickness [mm]	Si Filter thickness [mm]	Power absorbed in C Pre-filter [W]	Power absorbed in Si Filter [W]	Power absorbed in first Laue Xtal [W]	Power dump in beam stop [W]
2	0	3331	0	1642	2435
2	1	3331	2246	354	1477
2	2	3331	2840	177	1060
3.5	0	4057	0	1182	2169
3.5	1	4057	1691	310	1350

3.5	2	4057	2215	159	977
5	0	4560	0	907	1941
5	1	4560	1341	271	1236
5	2	4560	1803	143	902
10	0	5578	0	457	1373
10	1	5578	724	180	926
10	2	5578	1037	102	691

As can be seen from the results, even with the thickest C shielding, it would be rather difficult to work with a single 2 mm Si filter in front of the Laue monochromator, because of the very high heat load that would not be sustainable by a single Si blade. It would then be necessary to split the overall 2 mm Si over several thinner blades, similarly to what is done with the C pre-filters. Moreover, the white beam stop after the first crystal should probably be a sloped block made of GlidCop as the total power and, mostly, the power density is still high and because of space constraints it may not be possible to design the stop with a very shallow slope to the incident beam. Finally, even with the max. shielding (10 mm C + 2 mm Si), there are still ~ 100 W dump in the first crystal and the large amount of shielding material would make the device transmission not very efficient below 30 keV. Careful attention should then be dedicated to the matching of protective material thickness vs. overall transmission and vs. power loading of all elements (filters, crystal and beam stop), unless the beamline acceptance is significantly reduced. The envisaged system design will result in an extreme stable, massive and compact system. The vacuum chamber will directly sit onto a solid U-shaped granite block avoiding efficiently amplifications from floor vibrations. Based on our approach of in-vacuum solutions the monochromator mechanics will be placed inside the vacuum vessel. As a result the design will be very compact avoiding vacuum feed-throughs for any movements and the mechanics of all movements will be placed to the crystals as close as possible. Therefore, the system will prove to be very stable and precise and will yield the following advantages: The intended design for the monochromator will permit operation in the energy range of 20-100keV with a constant beam offset of 15 mm upwards. The following adjustment units are shown in Table .

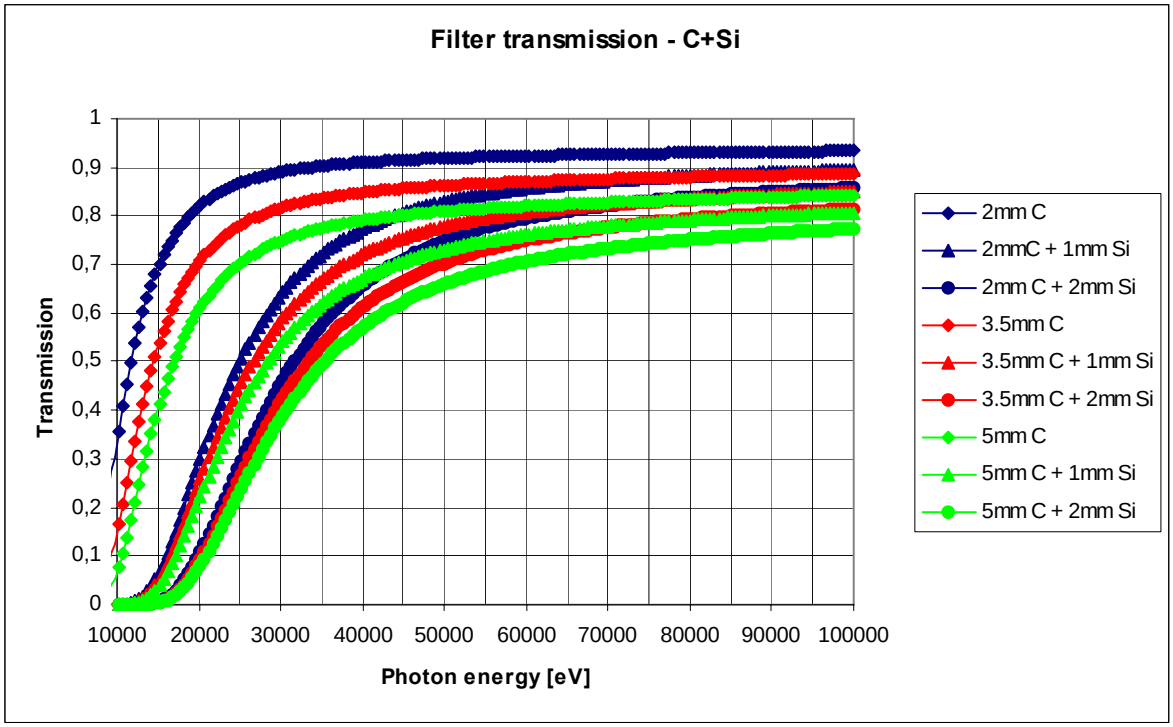

Figure 2: Transmission of various filter combinations on the powder diffraction beamline.

Table 6.15 Possible Adjustments for the Sagitally-Focusing Double-Crystal Laue Monochromator.
Bending adjustments are not shown in this table.

Movement	Range	Resolution	Repeatability
Whole optic assembly:			
Transversal (Y)	150 mm	≤ 5 µm	≤ 20 µm
1st and 2nd crystal units:			
Longitudinal (X)	500 mm	≤ 0.5 µm	≤ 20 µm
Yaw rotation (ϕ_1)	360°	≤ 10 µrad	≤ 10 µrad
Vertical (Z1)	40 mm	≤ 0.1 µm	≤ 5 µm
Roll rotation (χ_1)	-20 – 20°	≤ 10 µrad	≤ 20 µrad
Bragg rotation ($\theta 1_{coarse}$)	-5 – 35°	≤ 10 µrad	≤ 20 µrad
Bragg rotation ($\theta 1_{fine}$)	± 50 µrad	≈ 0.01µrad	≈ 0.06" (uni-directional)

6.4.3.4 White Beam Shutter

The white beam shutter is included in the front-end section (Section 6.4.1), and thus does not belong to the scope of supply for the beamline.

6.4.3.5 Vertically Focusing/Collimating Mirror

The basic design of the damping wiggler powder diffraction beamline foresees a single vertically collimating/focusing mirror placed in the front optical enclosure (white beam section), upstream of the sagitally-focusing double-crystal Laue monochromator. Nevertheless it has been decided to make provisions

for a possible upgrade of the beamline optics, leaving enough space in the beamline layout for the installation of a further horizontally/vertically focusing mirror (double toroid) downstream of this monochromator. Special attention has been paid to the cooling of the mirror, which is exposed to a significant level of absorbed power load and whose performance is rather critical in determining the ultimate energy resolution of the monochromator. An established technical solution for the mirror cooling, similar to the one that is implemented at the 7 Tesla superconducting wiggler HMI beamline at BESSY and at the Australian Synchrotron XAS beamline relies on indirectly cooling the mirror substrate with three Cu cooling blades immersed in a Ga-In eutecticum bath filling grooves machined in the optical surface of the mirror. This technical solution has already demonstrated to be able to cope with a total absorbed power load of the order of 2 kW but may fail for the even higher loads that the mirror may face at NSLS-II (Appendix D).

We have then explored two additional options that offer a better chance to withstand extreme heat loads: (i) Directly cooled Glidcop Mirror or (ii) Directly cooled Si Mirror. There is a possibility to use Glidcop as a mirror substrate material. This solution allows a direct cooling schema, which certainly has some advantages for higher power loads of a few kW (Appendix D). It should be noted that some doubts exist on the long term stability of Glidcop when exposed to the white beam and furthermore it is a more challenging material to polish than Si. A more favored direction is to use a directly cooled Si mirror. This technology is in use at beamlines at NSLS and the ALS and such mirrors can be realized with the requested quality. Provided that it is not directly exposed to the X-ray beam, the stability of the frit-bonding seems not to be a problem even after several years of use. Mirror specifications are shown in the table below.

Table 1 Specifications for the ACCEL vertically focusing/collimating mirror, for the powder diffraction beamline.

Mirror Substrate	Mono-crystalline Silicon (or Glidcop)
Direction of Reflection	Upwards
Shape	FLAT /cylindrically bent to tangential cylinder
Tangential Bending Radius	5.0 km - flat (> 40 km)
Sagittal Bending Radius	flat (> 1 km)
Substrate Length	approx. 1400 mm
Substrate Width	~ 120 mm
Substrate Thickness	60 to 70 mm**
Optical Active Surface: Length	1200 mm
Optical Active Surface: Width	2 x 35 mm (Si & Pt)
Sagittal Slope Error:	< 15 µrad rms
Tangential Slope Error:	< 2.5 µrad rms on 1200 mm (Best effort: < 2 µrad rms)
Micro Roughness	< 3 Å rms; best effort < 2 Å rms
Coating	Pt> 600 Å; Cr underlayer/ Bare central Si stripe
Cooling	Directly cooled

The ACCEL high stability mirror system mechanics is designed to be very robust, reliable and to allow easy access for maintenance and installation. A key design feature is that the mirror positioning mechanics is directly supported by a massive granite block that is mechanically decoupled from the vacuum chamber. This design allows to realize a very stable system and to greatly reduce the influence of vibrations propagating along the beamline. In order to get an as easy as possible access to the mirror, rectangular vacuum chambers are used. The chamber lid can be removed and then the entire mirror with its positioning mechanics is easily accessible.

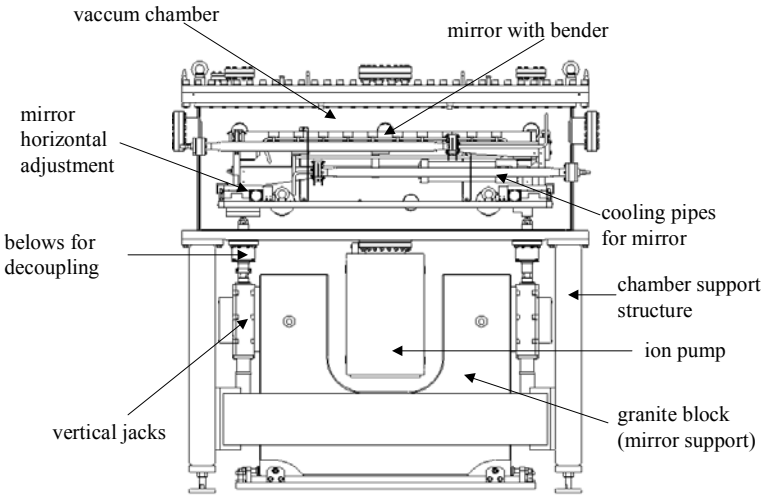

Figure 6.xx Side view of a high stability mirror system with a water-cooled bender.

Overall Technical Description. A very important design aspect of the high stability mirror systems is the complete mechanical separation between the optics and the vacuum chamber. This aims to avoid as much as possible vibration propagation to the mirrors. A massive granite block directly supports the mirrors holders/benders that are mechanically isolated from the vacuum chamber by means of edge-welded bellows. Another design guideline is to use in-vacuum actuators for the horizontal translation and its associated rotation (yaw), in order to (i) preserve the decoupling between the vacuum chamber with its support structure and the mirror with its positioner and (ii) to realize a system as compact as possible. Thus, two UHV compatible horizontal translation stages will be installed in the vacuum chamber (one at each extremity of the mirror), with one independent UHV compatible stepper motor each. Vertical translations will be performed by means of vertical jacks that also perform the two remaining rotations (pitch and roll). The mirror can thus be remotely adjusted in five independent degrees of freedom. All rotations (pitch, roll and yaw) will be realized by means of software pseudo-motors. Translations in/out of the beam will be realized by moving at the same time, of the same amount and in the same direction the three motors that act on the vertical jacks. Pitch and roll rotations will also be realized by the same three jacks. Horizontal translation (strip change) and yaw rotations will be realized by means of the two in-vacuum motors that act on the horizontal linear translation We suggest using a protective water-cooled steering mask between the mirror and the monochromator. It serves to better protect the monochromator interior or any un-cooled surface downstream from being hit by a mis-steered hot beam coming off the 1st mirror and further serves as a conductance limiting aperture for the vacuum performance between these two sections. To accommodate all operation modes of the beamline this mask has to sit on a vertical stage and will be equipped with edge welded bellows to allow for the necessary translations.

The mask will have water channels, I.D. 8 mm, with copper tubes brazed to it (no water-to- vacuum joints are used in our design). The material will be Glidcop and the impinging area will have a suitable slope so that it can withstand the high thermal stress that will be produced under worst conditions.

6.4.3.5 Beam monitoring elements

Beam monitoring elements are extremely important for beamline alignment. In this section, three such systems (as provided by ACCEL), are described: (a)Water-cooled White Beam CVD fluorescence screen The device consists of a retractable water-cooled CVD diamond foil, acting as x-ray screen, mounted to a pneumatic drive; the fluorescent effect is based on the residual doping with nitrogen atoms. The diamond screen is transparent, i.e. beam detecting further downstream is possible. The assembly is mounted to a

DN100 CF cross with one view port permitting a side view onto the screen. The pneumatic drive is equipped with limit switches. The vacuum feed-through is made of edge-welded bellows. The water lines are brazed to the screen support to avoid vacuum-to-water joints. The foil is clamped to the cooled support. The projection of the beam onto the 45° inclined foil will be monitored with a CCD camera. This system is capable of staying in the beam. However, because of the resulting absorption at photon energies below 10 keV, we advise to withdraw the screen when not in use. Moreover, to increase the lifetime of the foil and prevent overexposure of the camera, this screen should only be used at reduced power levels, i.e. in combination with some of the carbon filters. This screen has been installed at the high power wiggler beamline at the Australian Synchrotron Project.

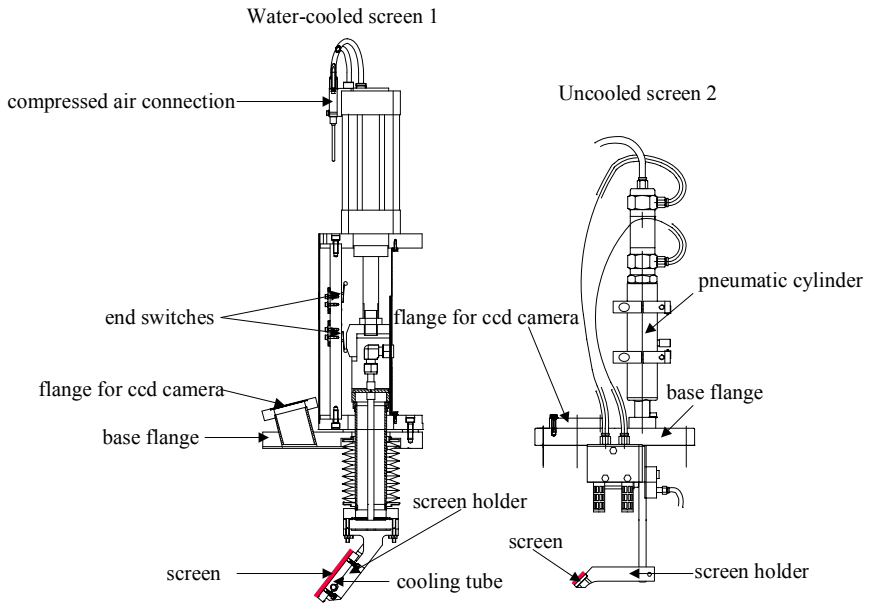

Figure6.xx Examples of ACCEL fluorescence screen beam monitors.

b) The fluorescence screen monitors typically are mounted to a pneumatic drive via a vacuum feed-through on a conflat flange. The water-cooled monitor is inserted in the beam by a stepper motor. The flange is also equipped with a view port for the camera that provides side view of the screen. Examples can be seen in Figure, for a water-cooled device and an un-cooled device.

c) Quadrant diode beam position monitor (4-diode BPM). ACCEL standard monitoring device for monochromatic beams of large size is a quadrant type detector that monitors the fluorescence yield of a target foil. Beam position information is derived from the intensity ratio of one pair of diodes. The device is rated for UHV and consists of a diode holder (holding four diodes) and a fluorescence foil holder. The four detecting silicon diodes are mounted to a vertical stage that permits the vertical positioning of the diodes which is necessary to operate the BPM at different beam heights.There are mounts for two foils, which can be of different kinds, or be the same. Typically, thin chromium and copper foils are used, but silver foils might be used as well. Chromium and copper have been working up to photon energies of around 20 keV. There is an option to mount a YAG crystal underneath this foil holder. Then, this YAG can be used to visualize the beam by means of a camera looking from the side onto a prism which is positioned behind the YAG. The assembly is designed such that it mounts to a CF100 flange and fits a standard size DN100 CF cross. The detection electronic for the diodes will be consisting of an integrated four-channel pico-ammeter with direct digital output.

d) The x-ray beam monitor is a commercially available visualization system for x-rays. Such a system provides a field of view large enough to study the beam size, beam profile and the beam position stability of a focused beam in the end-station (at atmosphere).

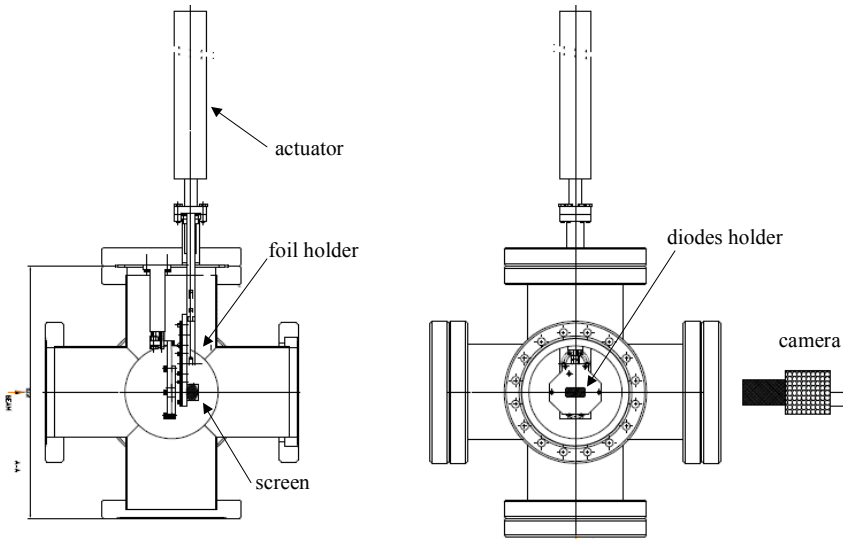

Figure 6.xx BPM (UHV rated) with diodes and fluorescent foil and screen.

6.4.3.6 Monochromatic Shutter

Although the powder-diffraction beamline anticipates using in-house fabricated monochromatic beam shutters, we include a description of the ACCEL photon shutter for completeness. These shutters consist of a high-density material absorber block, which is moved by means of a pneumatic actuator. The feed-through is mounted to a DN100CF flange. The motion of the pneumatic actuator is transferred to the absorber block through an edge-welded bellow, which has a guaranteed life time of 10^5 cycles. The absorber block is made of a Tungsten alloy having a Tungsten content of > 95% and a density of 17.5 g/cm³. The pneumatically driven actuator has a stroke of 60 mm. The pneumatic drive can be operated within a pressure range between 4 to 8 bar. The necessary magnetic valve is switched with a voltage of 24 V. The speed is adjustable by means of one-way restrictors. Each limit (upper and lower) of the stroke is indicated by two independent electromechanical switches. In case of failure (i.e. no power supply at the magnetic valve and no pressure at the pneumatic actuator), the shutter will close due to gravity. In Figure, we present a shutter that was recently designed for GM/CA-CAT (APS) and CMCF (CLS) where redundancy in form of double actuators was required.

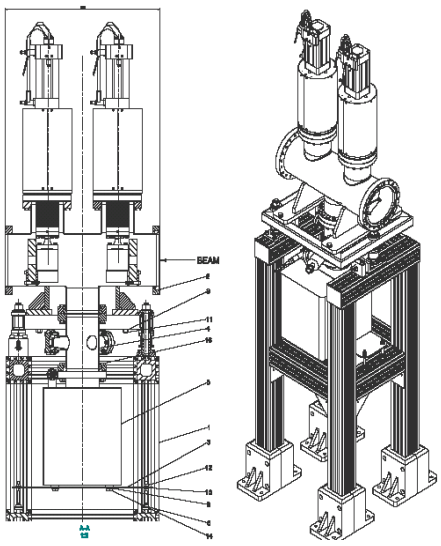

Figure 6.xx Sketch of one of ACCEL's monochromatic photon shutters.

6.4.3.7 Vacuum windows

A typical solution for the final widow in the powder diffraction beamline is to use a Be foil of appropriate aperture, diffusion bonded to a stainless steel double sided flange. The exit Be window will be carbon coated to protect the beryllium surface against oxidation in air.

Table 6.xx Specifications for the final Be window in the powder-diffraction beamline.

General:	
Material	stainless steel flange
	CF100
Foil material	Be-foil, PF-60, both sides polished
Foil thickness	0.250 mm
Aperture size of Exit window	tailored

6.4.3.8 Enclosures

There will be three beamline radiation enclosures at the damping wiggler powder diffraction beamline; one first optics enclosure (FOE) and two experimental hutches. The FOE contains all beamline optics (filter units, mirror, monochromator, beam monitoring assembly and photon shutter), and will be a white beam hutch. The FOE with its lead shielded sides interfaces to the ratchet wall of the storage ring. Following the standard regulations for white beam hutches, the labyrinths to run electricity as well as media and power connections will be located on the roof. The hutch will be very long (approx 17 m) to accommodate the optics for both the original beamline and possible optics for a canted beamline. One double door with sliding panels, large enough to move in larger components using a fork lift, will provide access to the hutch. Based on our experience with regulations at national US laboratories and following the ALARA practice we have based our evaluation for the FOE on the more conservative numbers for lead shielding that are presented in the document, NSLS-II Technical Note 014, Table 6, i.e. following the thickest lead shielding requirements for the FOE (see details below). The beam transport between the FOE and the first experimental hutch will be a tunnel type (coffin style) transport. Such an enclosure design will provide enough flexibility to accommodate vacuum pipes for beamlines. The shielding of interfaces such as guillotines etc. is included. All three

enclosures will be equipped with an overhead crane (one metric ton), several labyrinths and sliding doors. A summary of the specifications is as follows:

First Optics Enclosure, white beam hutch (FOE):

	Upstream wall 2 m x 3.3 m	Sides 17.5 m x 3.3 m	Downstream wall 3 m x 3.3 m	Roof 17.5 m x 2.5 m
Shielding requirements Lead [mm]	16 mm	23 mm	50 mm	14 mm

- one extra panel of size 1 m x 1 m x 50 mm at downstream wall centred at 1400 mm above floor
- one sliding double door (white beam hutch)
- 10 times chicane on the roof, all chicane with hinges
- one hutch crane, 1 metric ton
- one set of guillotine, adjustable shielding around beam pipe on downstream wall
- painted with primer

Shielded Beam Transport (coffin style, base with lid):

Lead shielding of 7 mm thickness.
Dimensions: 2 m long, 0.4 m x 0.4 m cross section
Support stands every 2 m with gussets.
Painted with primer

Upstream Experimental Enclosure, monochromatic hutch (EH-1):

	Upstream wall 4 m x 3.3 m	Sides 7 m x 3.3 m	Downstream wall 4 m x 3.3 m	Roof 7 m x 4 m
Shielding requirements Lead [mm]	6 mm	6 mm	6 mm	5 mm

- One sliding door
- 5 times chicane on the roof, 3 times chicane on the sides, all chicane with hinges
- one hutch crane, 1 metric ton
- one set of guillotine, adjustable shielding around beam pipe on upstream wall
- painted with primer

Downstream Experimental Enclosure, monochromatic hutch (EH-2)

	Upstream wall 4 m x 3.3 m	Sides 7 m x 3.3 m	Downstream wall 4 m x 3.3 m	Roof 7 m x 4 m
Shielding requirements Lead [mm]	6 mm	6 mm	6 mm	5 mm

- One sliding double door
- One sliding single door
- 5 times chicane on the roof, 3 times chicane on the sides, all chicane with hinges
- one hutch crane, 1 metric ton
- one set of guillotine, adjustable shielding around beam pipe on upstream wall
- painted with primer

Provision will be made to run cable trays and utilities inside and outside the hutches.

6.4.4 Instruments

This section describes the end-station instrumentation necessary to perform high-energy high-resolution powder diffraction. The scope of the powder diffraction beamline allows for one end-station (Endstation 1), that will allow high-energy high-resolution powder diffraction, with the other optical enclosure (most upstream enclosure) to be populated in the future – possibly by existing NSLS-I equipment and served by a canting wiggler source in the high-β straight-section.

6.4.4.1 Endstation 1

This section describes the high-energy high-resolution powder diffraction end-station. Our current thinking in designing this facility is to use equivalent set-ups employed at various high-energy high-resolution powder diffraction stations at other synchrotron radiation facilities. In general, the end-station consists of a highly accurate 3-axis diffractometer: One axis is used for sample orientation (or spinning), the second axis holds a fast read-put position sensitive silicon strip detector for in-situ time-resolved studies and remains essentially fixed, and the third axis is used to hold a multi-crystal silicon array analyzer system that can be rotated in the vertical diffraction plane. The scientific drivers for this particular instrument has been outlined in the first two sections of this chapter. Two high-resolution diffractometers, whichexist at various high-resolution powder diffraction beamlines, could be employed at this beamline.. We show two multi-channel crystal arrays on the drawing (Figure 14, taken from the SLS design), but a different design and large array could be easily envisaged. The resolution of the rotary stages need to be highly accurate to obtain accurate peak positions and reliable data. The Newport and RPI systems have the necessary resolution to enable the operation of this facility. The other all resolution of the system should provide peak shape resolution of < 5 milli-degrees, thus allowing accurate peak profile measurements essential in the study of strain, microstructure and lattice defects. Mython strip array detectors (PSI design) are to be installed at the DIAMOND, SLS and Australian synchrotron facilities and our design will incorporate similar technology; a 7000-element silicon strip detector array currently being fabricated at the NSLS for in-situ real time material studies. A variety of sample environments (not shown) has been included in our budget, consisting of cryostats, furnaces, laser heating and diamond-anvil cells for high-pressure research. In addition, a robotic sample chamber has been included (not shown) for high-throughput measurements for combinatorial investigation and screening purposes. The overall design is relatively standard, except for the inclusion of a graded bendable multiplayer system that will be used to focus the beam to ~ 14 microns in the horizontal for studying small samples (e.g. for high-pressure diamond-anvil cell research). This mirror is located relatively close to the sample position to minimize beam motion as the multiplayer is rotated to match the incoming x-ray wavelength.

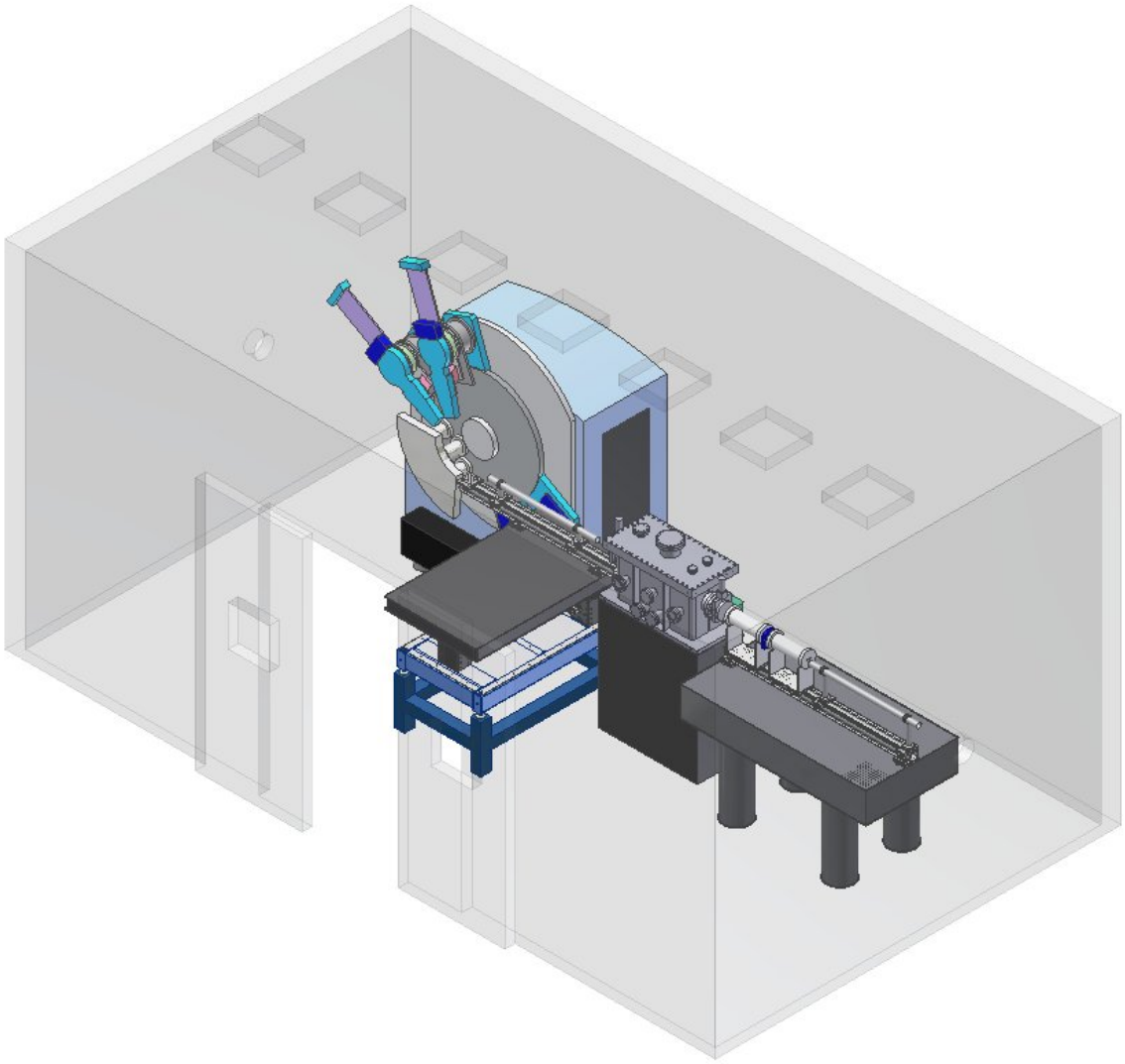

Figure 3: Conceptual design of the NSLS-II high-energy high-resolution powder diffraction beamline. For clarity, sample environments (such as crysostats, furnaces and diamond-anvil cells) and a robotic sample changer for high-through-put applications are not included in the figure.

6.4.4.2 Endstation 2

Although not in the scope of the present NSLS-II project, the most upstream optical enclosure is included to serve as a possible second powder diffraction beamline. This second beamline, which could be served by a canted wiggler source in the high-β straight section, could be populated by existing NSLS-I equipment. For example, there are many Huber diffractometers, several CCD cameras and robotic sample changers operational at NSLS beamlines at this current period of time.For example, we show in Fig XXX, a routine powder diffraction setup, with a huber diffractomer, with a ccd camera on a 2-theta arm. We anticipate such a facility would also be in high demand at the NSLS-II machine.

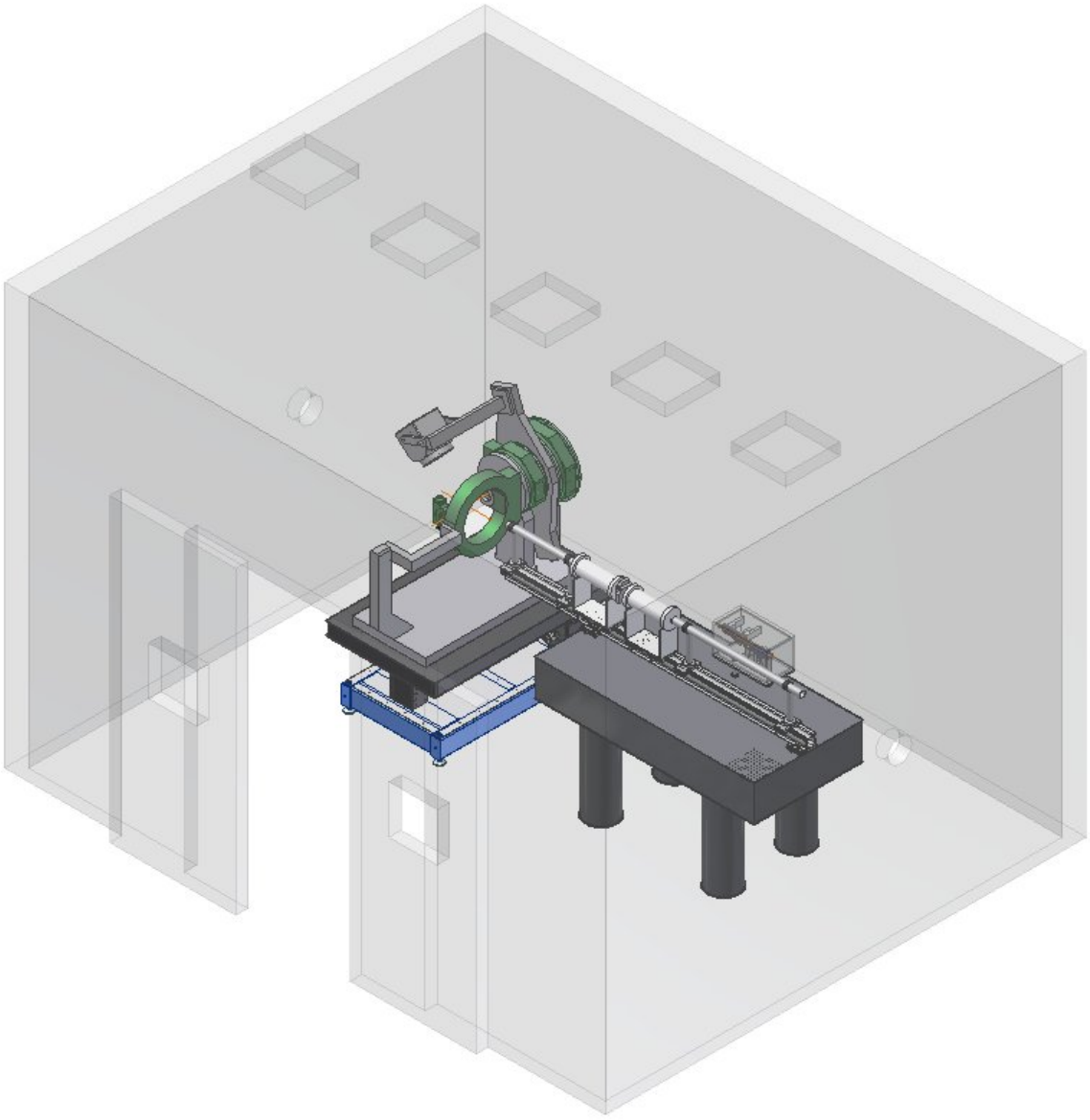

Figure 4 Conceptual layout for a second powder diffraction beamline, upstream of the high-energy high resolution NSLS-II powder diffraction beamline. Note that this end-station is not in the current scope of the NSLS-II project.

6.5 Additional Requirements Imposed on the Conventional Facilities

Powder diffraction experiments will be performed in both the high-resolution (crystal array) and area detector modes. The crystal analyzer is the most demanding in terms of angular stability, since it aims to provide high d-spacing resolution and precision. The area detector mode is primarily affected by position stability. Both modes are sensitive to beam energy changes.

In the crystal analyzer mode, the critical requirement is angular stability. A typical powder peak width using an analyzer crystal is in the range of 0.001^{o} to 0.01^{o} at 17 keV, depending on the sample quality. 0.001^{o} is unusually good. Let us consider 0.005^{o} as typical. Then, the photon beam stability should be 10% of this value i.e. 0.0005^{o}, or 8 μrad.

A related concern is the energy stability, since energy maps directly to d-spacing in a diffraction experiment. Using Si(111), it's intrinsic energy resolution, $dE/E \sim 10^{-4}$, which sets a limit on what we can achieve with a sample. If we assume we can find centroids to a few percent of this, we end up with an energy stability requirement of at least 10^{-5}. This maps to an angular stability of 1 or 2 μrad [Si(111) at 17 keV has a Darwin width of 15 μrad], and a monochromator temperature stability of 10 Kelvin.

All of the above arguments are directed in the vertical plane of diffraction.

Area detector measurements are typically 10 times or more lower resolution than using a crystal analyzer, so angular stability is not the limiting case. In contrast to the crystal analyzer mode, position stability is important, since position is used as an angle analogue. If we assume a focused beamline with a focal spot of 100 μm and a detector with similar spatial resolution, then using the '10% rule', beam stability should be on the 10 μm level. Similar arguments apply to energy stability. In this case, the spatial stability requirements are in both the horizontal and vertical directions.